Biophysical Aspects of Binding Interactions between Anticancer Drugs and G-Quadruplex DNA

A thesis submitted to

Indian Institute of Science Education and Research Pune

in partial fulfilment of the requirements for the

BS-MS Dual Degree Programme

Thesis Supervisor: Dr. Partha Hazra

By

Vivek Kumar

20091024

April, 2014

IISER PUNE

Indian Institute of Science Education and Research, Pune

Pashan, Pune, India 411008.

Certificate

This is to certify that this dissertation entitled "***Biophysical Aspects of Binding Interactions between Anticancer Drugs and G-Quadruplex DNA***" towards the partial fulfilment of the BS-MS dual degree programme at the Indian Institute of Science Education and Research, Pune, represents original research carried out by *Mr. Vivek Kumar* under the supervision of *Dr. Partha Hazra*, *Chemistry* during the academic year 2013-2014.
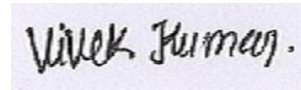
Date: 01/04/2014

Place: IISER, Pune

Signature

Declaration

I hereby declare that the matter embodied in the report entitled "***Biophysical Aspects of Binding Interactions between Anticancer Drugs and G-Quadruplex DNA***" are the results of the investigation carried out by me at the department of Indian Institute of Science Education and Research, Pune, under the supervision of Dr. Partha Hazra and the same has not been submitted elsewhere for any other degree.

Date: 01/04/2014

Place: IISER, Pune

Signature

Acknowledgements

Contents

List of Tables

Abstract

Biophysical Aspects of Binding Interactions between Anticancer Drugs and G-Quadruplex DNA

The G-quadruplex (GQ-DNA), an alternative structure motif of DNA, has emerged as a novel and exciting target for anticancer drug discovery. GQ-DNA structure formed in G-rich sequence in presence of monovalent cations such as Na^+/K^+. At the end of human telomeric sequence consisting of tandem repeat of TTAGGG single stranded DNA sequence forms G-quadruplex. GQ-DNA formed by human telomeric DNA at the chromosomal end is the point of interest due to their direct relevance for cellular aging and abnormal cell growths. Small molecules that selectively target and stabilize G-quadruplex structure(s) may serve as potential therapeutic anticancer agents. In this work, we have studied the interaction of proflavine and harmine with human telomeric DNA sequence. Spectroscopy and calorimetric studies indicate that association of proflavine (PF) with GQ-DNA is an enthalpically as well entrophically driven phenomenon with a 3:2 (PF:GQ-DNA) stoichiometry and the binding of PF to GQ-DNA is characterized by intrinsic association constants of ~1 $\times 10^6$ M^{-1}. PF binding with G-quadruplex induces G-quadruplex structure more towards parallel structure. When GQ-DNA complexes with PF, it gains extra stabilization, which is reflected from the rise in melting temperature of ~8^0C. With observed binding stoichiometry (PF:GQ-DNA = 3:2) from isothermal titration calorimetry (ITC) and job's plot, we propose that one molecule of proflavine (PF) gets sandwiched between two molecules of GQ-DNA, and two PF molecules are stacked to each of the two remaining ends of GQ-DNA.

In the case of study of interaction between harmine and GQ-DNA, we have observed that a noteworthy decrease in absorption and severe quenching in fluorescence intensity upon addition of GQ-DNA. This observation indicates a strong binding interaction between harmine and G-quadruplex. It is further supported by excited state time-resolved measurements. Increase in hydrodynamic radius of harmine bound GQ-DNA compared to drug alone (calculated from time-resolved anisotropy data) confirmed a complex formation between harmine with GQ-DNA. We have calculated the binding stoichiometry of the complex from Job's plot and we

have found 3:2 (harmine:GQ-DNA) binding stoichiometry. Presently, we are also trying to get insight into the thermodynamics of this binding process with the help of ITC measurements.

1. INTRODUCTION

Living in an era of upraising cancer threats, one of the prime focuses of modern science is anticancer drug developments and its application towards a hazard free humanity. A countless number of drugs[1] are known either to intercalate or bind to groove which results inhibition for DNA replication and hence cell division. Not only the canonical genomic DNA but several non-canonical DNA structures are also treated as potential targets for anti-cancer drugs.[2] Among various non-canonical DNA motifs, a special kind known as G-quadruplex demands burgeoning attention since discovery of tetramer guanosine residue by Gellert *et. al.* in 1962[3]. G-quadruplex is a four-stranded DNA (GQ-DNA) structure, having stacked G-quartets held together by eight Hoogsteen hydrogen bonds (**Figure 1**).[2-4] G-quadruplex
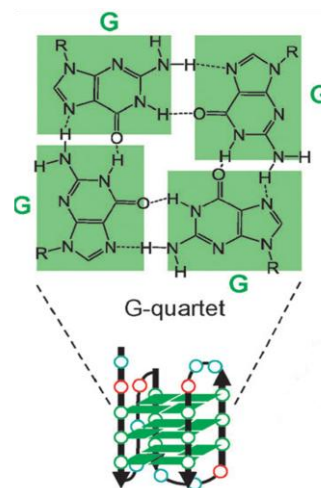
Figure 1. G-quadruplex

formed mainly in G-rich DNA sequences like promoter region of some proto-oncogenes for example C-MYC, C-KIT, KRAS and at human telomeric end.[5] The quadruplex sequences are well known to stabilize in presence of metal ions. During this metal ion assisted folding of G-quadruplex it shows polymorphism.[4, 6] The structural diversity of G-quadruplex DNA is largely dependent over its sequence as well as experimental conditions (**Figure 2)**[4]. Interestingly folding of specific DNA sequence into G-quadruplex structure of different topology depends not only over the types of cations (such as Na^+, K^+), but also over small molecules, or certain cationic dyes [6b, 7].

	Monomer								Dimer			Tetramer
	Antiparallel			Parallel	Mixed			Antiparallel		Parallel	Mixed	Parallel
Sequences	d[AG$_2$ (T$_2$AG$_3$)$_3$]	d(G$_2$T$_2$G$_2$ TGT G$_2$T$_2$G$_2$)	d[(G$_3$T$_2$A)$_3$ G$_3$T]	d[AG$_2$ (T$_2$AG$_3$)$_3$]	d[(T$_2$AG$_3$)$_4$ T$_2$]	d[(G$_3$T$_2$ A)$_3$ G$_3$T]	d[G$_3$T$_2$C AG$_2$]	d[G$_4$T$_4$G$_4$]	r[UAG$_3$U$_2$ AG$_3$U]	d[{GIG(T$_2$ AG$_3$)2T] d[TAG$_3$U]	d[T2G4T]
Metal ions	Na$^+$	K$^+$	K$^+$	K$^+$	K$^+$	Na$^+$	K$^+$	K$^+$	K$^+$	K$^+$	K$^+$
PDB ID	143D	148D	2KF7	1KF1	2JPZ	2KF8	1F3S	1JPQ	2KBP	2AQY	139D
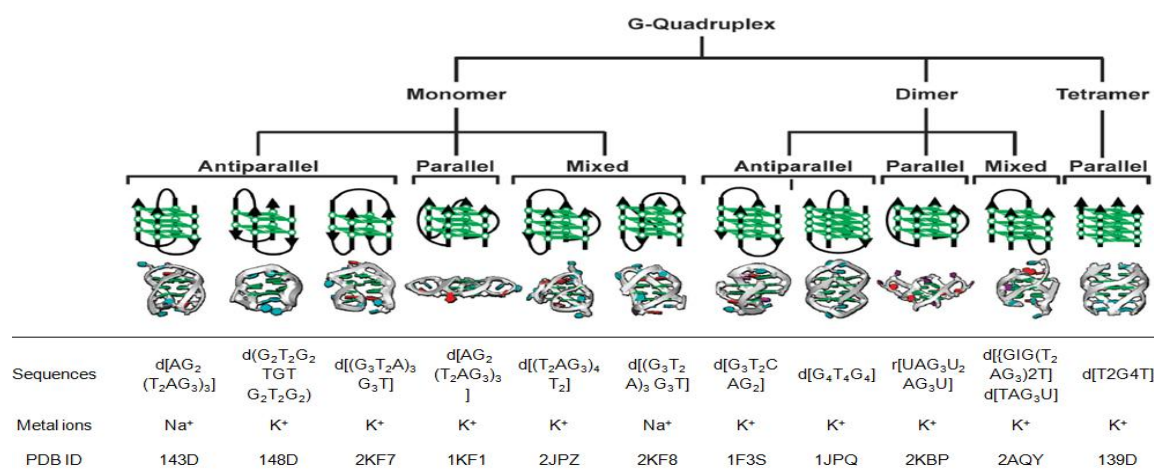
Figure 2. Polymorphic G-quadruplex.[4] Different structures stabilized in presence of metal ions.[4]

Telomere is a segment of DNA occurring at the ends of chromosomes in eukaryotic cell (Figure 3). Human telomeres are usually of 5-8 kb in length, formed by 5′-TTAGGG-3′ tandem repeats. The bulk portion of telomeric DNA adopts a double-helical conformation keeping G-rich sequence paired with C-rich complimentary sequence. However, the 3′ end of such telomeric DNA resides overhang as single stranded G-rich DNA of approximately 100-200 bases in length (**Figure 3**). These single stranded DNA has very high affinity to fold into a G-quadruplex structure in presence of small cations such as Na^+, K^+, etc (**Figure 2**). Typically, Na^+ induces antiparallel structure while K^+ induces a mixed population of both parallel and antiparallel structure of human telomeric G-quadruplex DNA[4, 6b](**Figure 2**). Telomeric G-quadruplex structures have received widespread attention because telomere plays an important role in cellular ageing and cancer[8].
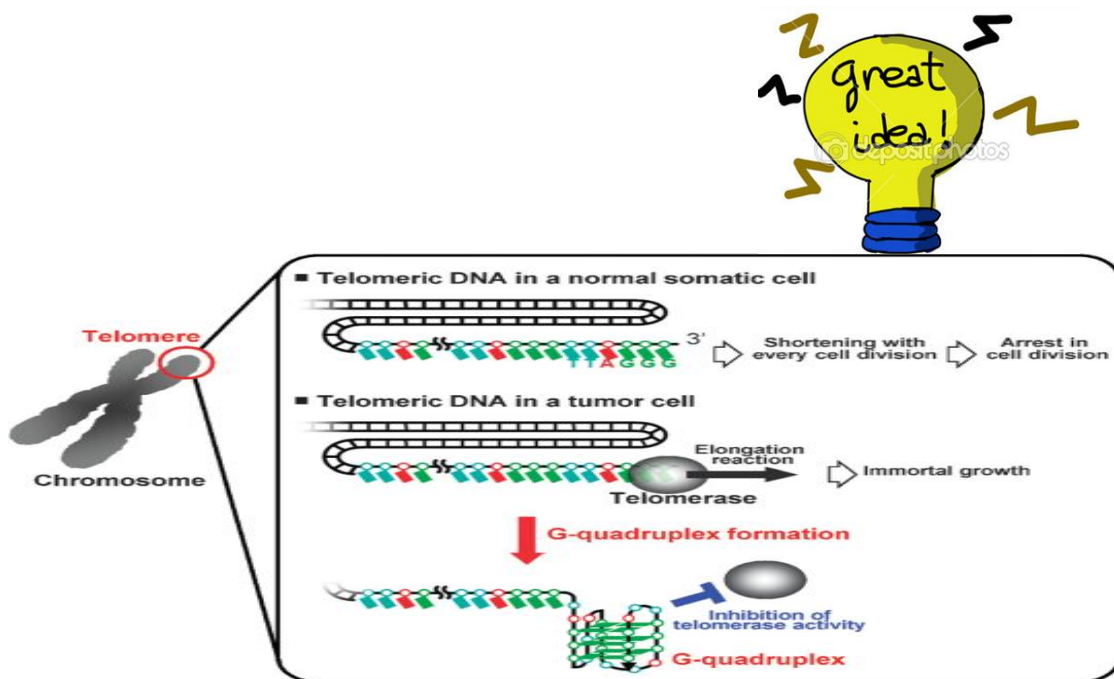
Figure 3. Biological role of telomeric DNA and telomerase.[4]

1.1. Telomerase:

DNA in the cell nucleus is copied by an enzyme known as DNA polymerase. A DNA polymerase makes a new DNA strand (the process known as replication) from $5^{'}$ to $3^{'}$ direction, by adding a free nucleotide onto the growing $3^{'}$-end of new strand. DNA replication is a semi-conservative process in which the replication of

overhanging terminal ends (lagging strand) of chromosome cannot be accomplished by conventional DNA polymerase.[9] Because of the inability to replicate ends of the chromosome, telomere would progressively gets shorter and shorter in each cycle of DNA replication.[4, 10] The telomeric sequence shrinks with each cycle of replication and quickly results in the loss of vital genetic information, which is needed to sustain a cell's activities. As a result, the chromosomes become less stable, leading to cellular dyefunction and cell death. However, the end replication problem is solved by an enzyme called telomerase, a ribonucleoprotein.[9, 11] Telomerase recognises the tip of existing G-rich telomeric sequence (TTAGGG) using a RNA template within the enzyme telomerase, and extends the DNA strand in 5′ to 3′ direction (**Figure 4**). This extended lagging strand now provides the necessary template for completing synthesis of the remaining DNA by DNA polymerase. Thus, telomerase plays a crucial role in making chromosome stable by compensating partially the loss of telomeric DNA during DNA replications.
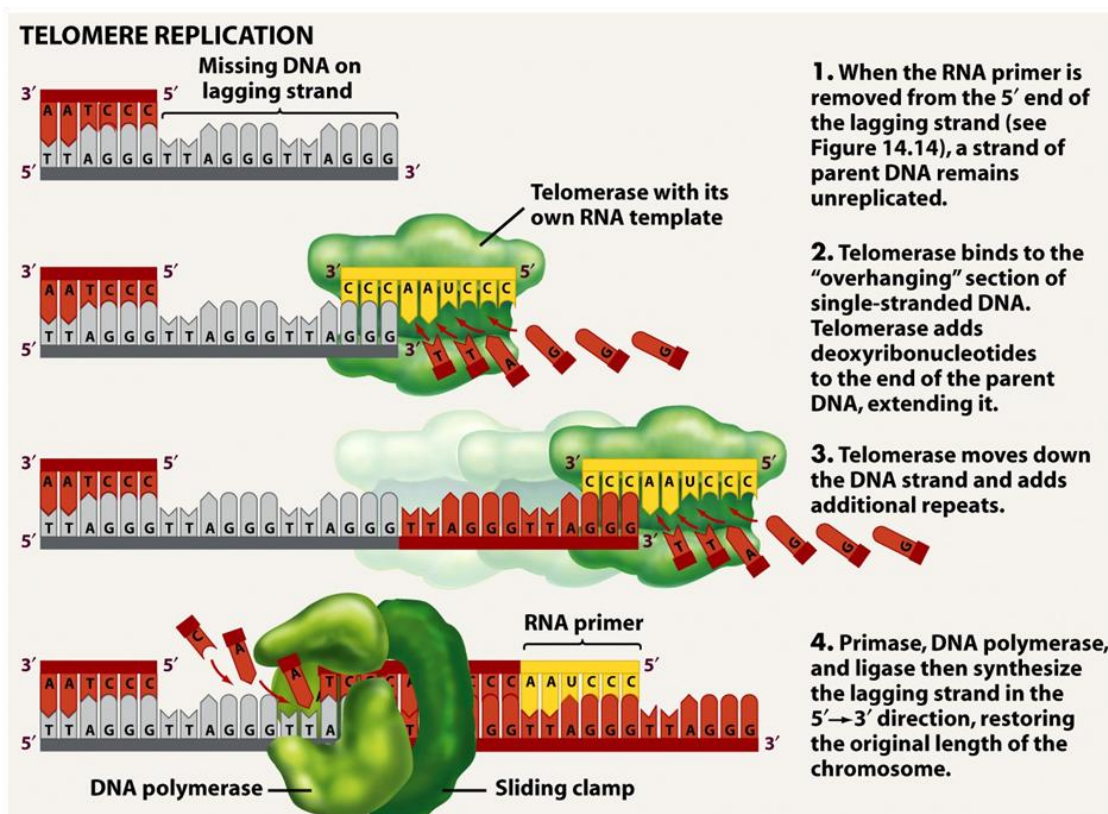
Figure 4. Telomerase and it's role in elongation of telomeric DNA sequences.[12]

Telomerase expression is tightly controlled in normal somatic cells in which the telomere become shorter during each round of cell division. Therefore, the length of the telomeric DNA sequence and the rate at which it get shorter in each cycle of DNA replication (cell division) determine the age of a particular cell. Consequently, these progressive decreases limit the proliferation potential of cells, whereas, 80-85% human tumor cells having functional telomerase that keep elongated telomeric DNA and hence it leads to an abnormal growth of cells (cancer)[13]. Inhibition of telomerase and the related telomere shortening is key strategy for development of anticancer agents. Formation of stable telomeric G-quadruplex DNA (GQ-DNA) can resists the telomerase activity (**Figure 3**), as it cannot function as a potential substrate for the enzyme. Though there are reports that G-quadruplex forming sequences are also present in the promoter region of some proto-oncogenes for example C-MYC, C-KIT, KRAS, etc. Among these, G-quadruplex formed by human telomeric DNA at the chrosomal end[5d, 5e, 6b, 14] is the point of interest due to their direct relevance for cellular aging and abnormal cell growths[8].

Small molecules and/or ligands (**Scheme 1**) that recognize and bind to G-quadruplex in telomeric DNA are celebrated as potential anti carcinogens.[4, 15] The very basic requirements for a molecule to be a G-quadruplex stabilizer is mainly three; (i) a heteroaromatic ring capable of π-staking interaction with nucleobases, (ii) a planner structural part which can fit over G-quatret plane and (iii) a cationic center which acts as initiator through electrostatic interaction with phosphate backbone of DNA[15a, 16]. Among various such kinds of molecules, we have studied the binding interaction of proflavine (PF) and harmine with G-quadruplex DNA and its effect over GQ-DNA structural stabilization. We have used steady state and time resoled fluorescence, circular dichroism (CD) and isothermal titration calorimetry (ITC) to explore the structural impact and the thermodynamics influences due to small the binding of planar anticancer drugs.

Phthalocyanine's derivative   Telomestotin's derivative   Daunomycin   Barberine
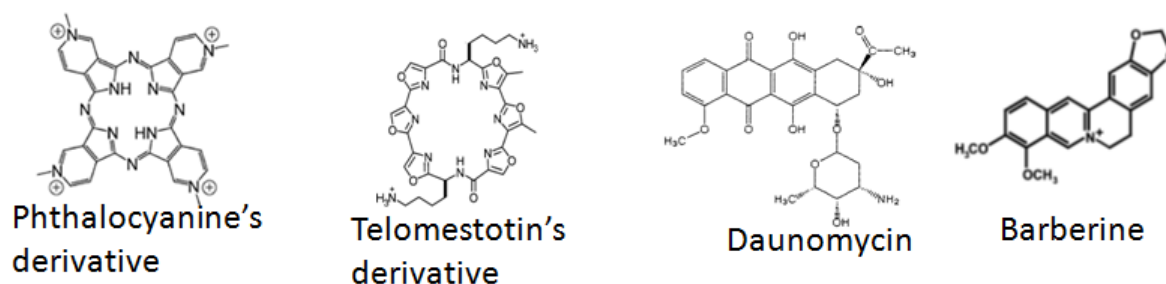
Scheme 1. Structure of molecules shown anti-telomerase activity.

1.2. Proflavine:

Proflavine (acridine-3,6-diamine) is an acridine derivative. Acridine and its derivative belongs to the polynuclear N-hetroaromatic family and have number of significant pharmaceutical uses[17]. Therefore, interaction of acridines with DNA has been studied extensively. For a prolonged duration acridines are well known to as intercalator in double stranded DNA and established as mutagenic as well as anti-carcinogenic[18]. The intercalation of acridine and its derivatives with DNA leads to inhibition of topoisomerase action that prevents important intracellular process like replication, transcription and repair[19]. Therefore, many of the acridine derivatives are well used in chemotherapeutic agents[20]. Although a bulk of literatures are found regarding several acridine derivatives interacting to double stranded DNA,[18] but study regarding interaction of proflavine (PF) with GQ-DNA is scarcely available. Understanding of proflavine interaction with non-canonical forms like G-quadruplex DNA might provide new insight towards understanding of potential telomerase inhibitor activity of PF.

Figure 5. Different prototropic forms of proflavine.

Literature reports on photophysics of proflavine shows that both absorbance and fluorescence spectra strongly depends upon the nature of the species formed and surrounding environment in their respective ground state and excited state[21]. Lowest excited singlet state of proflavine in hexane solution is strongly n-π* in character whereas in polar or polar protic solvents like alcohol/water the lowest excited state is clearly π-π* in character[22]. An increase in polarity of the solvents leads to a blue shift in absorption and red shift in emission spectra[21]. Since proflavine having higher dipole moment (2.72 D) in excited state than ground state(1.62 D)[21] leads to more stabilisation of excited state than ground state in polar solvent, hence, red shift in emission and blue shift in absorption are observed. In the present study we used mainly the photo-induced emission of protonated PF (pKa = 9.5, **Figure 5**.) in steady state and time resolved technique to explore its interaction with GQ-DNA.

1.3. Harmine:

Harmine (7-methoxy-1methyl-9*H*-pyrido[3,4-*b*]indole) is a natural alkaloid from β-carboline family. Harmine is generally isolated from plants like P. Harmala[23] , mostly found in eastern Mediterranean region and central Asia, North Africa and Middle East.

Harmine has many biological and pharmacological interests.[24] It has recently drawn attention due to their anticancer activities. It has been shown that harmine interact with DNA via both groove binding as well as intercalative mode and cause major DNA structural changes[25]. Harmine inhibits the activity of topoisomerase, and thereby, prevents important intracellular process like replication, transcription and repair.[25-26] Harmine is also associated with inhibition of the protein kinase DYRKIA. Over expression of DYRIA has been implicated in multiple diseases like tumergenesis, and uncontrolled cell proliferation[27]. In addition to that, it has been recently shown that harmine can reverse resistance to anticancer drugs (Camptothecin and Mitoxanthrone) by inhibiting the breast cancer resistance protein (BCRP)[28] which is responsible for multidrug resistance. Although a bulk of literatures are found regarding interaction of harmine with double stranded DNA and proteins, but there are no such studies reported with G-quadruplex.
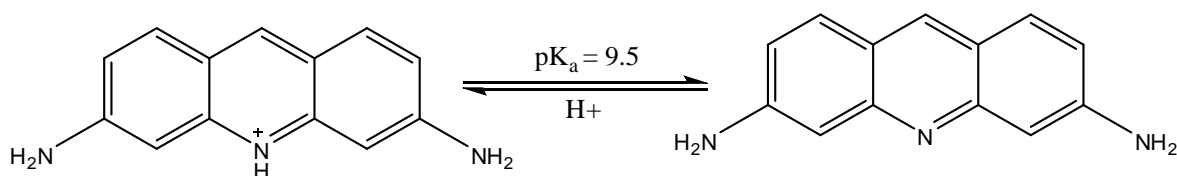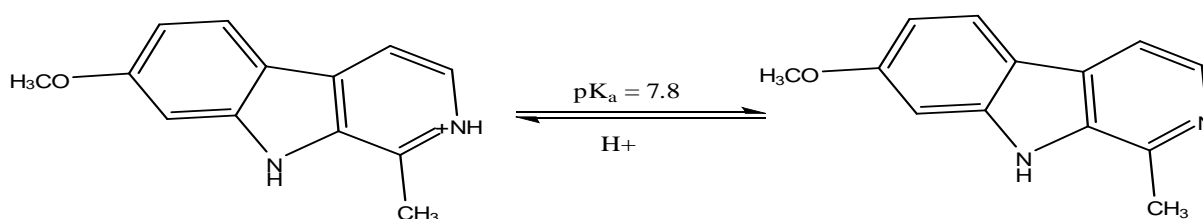

Figure 6. Different prototropic forms of harmine.

Literature reports on photophysics of harmine shows that both absorbance and fluorescence spectra strongly depends upon the nature of the species formed and surrounding environment in their respective ground state and excited state[29]. It was observed that harmine exists in equilibrium between neutral and cationic form in protic solvents like methanol and water. At lower pH = 7, it exists exclusive in cationic form and shows absorption and emission maxima at 320 nm, and 400 nm respectively. Between pH = 7 to pH = 9.5 both cationic as well as neutral form exist,

as its pKa value is 7.8 (**Figure.6**), and above pH = 9.5 only neutral form exists[30]. Although at higher pH only neutral form exists in the ground state, two emission bands appears: the neutral form emission (350 nm) and the zwitterions form emission (500 nm). Excitation spectra study reveals that zwitterions is formed exclusively in the excited state as result of double proton transfer process from neutral form via either N*→Z* and/or N*→C*→Z*.[30] The presence of several protophilic and protophobic functional groups (pyridine nitrogen and pyrrole nitrogen) is responsible for the existence of different forms of harmine at different pH. In the present study we have used mainly the photo-induced emission of protonated harmine (pH = 6.8) in steady state and time resolved fluorescence techniques to explore its interaction with GQ-DNA.

1.4. <u>Motivation of the Present Work:</u>

Looking the structure of protonated proflavine and harmine, these seem to have high possibility that proflavine and harmine can bind to G-quadruplex because it has (i) heteroaromatic ring capable of pi-staking interaction with nucleobases, (ii) a planner structure which can fit over G-quartet plane and (iii) a cationic centre which is necessary to involve in electrostatic interaction with phosphate backbone of DNA[15a]. Herein, we probe G-quadruplex and drugs association through steady sate and time resolved fluorescence spectroscopy to explore the effect of stabilization of GQ-DNA by an extrinsic non-covalent fluorescent marker. The structural modifications of G-quadruplex upon binding are highlighted through Circular dichroism (CD) spectra. A very detailed insight of thermodynamics of the interaction has been provided though Isothermal titration calorimetry (ITC) studies. The thermodynamic parameters obtained from steady-state anisotropy and ITC helps to gain the knowledge about the nature as well as driving forces of binding. Present work shows proflavine can act as a telomere G-quadruplex stabilizer through an entropically as well as enthalpically feasible process with high binding ability, and can be further used as an anti-carcinogenic molecule for the same. From steady-state and time-resolved spectroscopy techniques, harmine is also believed to be involved in strong stacking interaction with GQ-DNA.

2. **MATERIALS, METODS AND INSTRUMENTATION**

The 24-mer human telomeric (H24) DNA (5′-TTAGGGTTAGGGTTAGGGTTAGGG-3′) was purchased from Integrated DNA Technologies (IDT) and was used as received. Stock DNA solution was prepared by dissolving in 5 mM KH_2PO_4 and 5 mM K_2HPO_4 (pH=6.8) containing 150 mM KCl (PBS). All experiments and sample preparations were carried out in autoclave Millipore water. Before experiments G-quadruplex (GQ) DNA in PBS was annealed at 90 ^{0}C for 10 minute and stored at 4 ^{0}C for 48 hrs. The concentration of GQ-DNA was determined by the absorption at 260 nm through UV-visible spectrophotometer (Shimadzu UV-2600) at 25^{0}C using the molar extinction coefficient at 260 nm of ~2,44,600 $M^{-1}cm^{-1}$. Before doing any experiment, the formation of (3+1) hybrid G-Quadruplex (GQ) structure was confirmed through CD. The concentration of GQ is expressed in term of the oligomer, unless otherwise specified. Proflavine (acridine-3,6-diamine) and Harmine were purchased from Sigma-Aldrich and used without any further purification. The drugs were dissolved in the same buffer and concentration was determined by the UV-visible spectrophotometer (Shimadzu UV-2600) using the molar extinction coefficient 41,000 $M^{-1}cm^{-1}$. Due to less solubility of harmine in water, a highly concentrated stock sample was made in DMSO, so that in all the experiments, the DMSO content kept below 0.5% (v/v).

Absorbance measurements were performed in Shimadzu UV-2600 UV-Vis. spectrophotometer, and steady-state fluorescence spectra were recorded in FluoroMax-4 spectrofluorimeter (Horiba Scientific, U.S.A.). Time-resolved fluorescence decays were collected on a time correlated single photon counting (TCSPC) spectrometer (Horiba Jobin Yvon IBH, U.S.A.). In TCSPC, we have excited drugs at its absorption maximum using, 444 nm diode laser (440 nano-LED, FWHM = ~200 ps) and 325 nm diode (325 nano-LED, FWHM = ~200 ps) for exciting proflavine and harmine respectively. The fluorescence signal were collected at magic angle using a MCP-PMT (Hamamatsu, Japan) detector at respective emission maxima. For time-resolved anisotropy study, we have used motorized polarizer in the emission side. The emission intensities at perpendicular (I_{VH}(t)) and parallel polarization (I_{VV}(t) were collected alternatively for 60 s. For typical anisotropy decay, the difference between the peak counts at parallel and perpendicular polarization

was kept to 3000. The analysis of lifetime and anisotropy was done by IBH DAS6 software. We have fitted both life-time as well as anisotropy data with a minimum number of exponential. Quality of each fitting was judged by χ^2 values and the visual inspection of the residuals. The value of $\chi^2 \approx 1$ was considered as best fit for the plots.

Circular dichroism (CD) spectra were recorded on a J-815 CD (JASCO, U.S.A.) at 25^0C. The data was collected from 200 to 350 nm at every 1 nm with band width 1 nm. All measurements were taken in 0.2 cm path length cuvette with 300 µL sample volume. Each CD profile is an average of 3 scans of the same sample collected at a scan speed 100 nm/min, with a proper baseline correction from the blank buffer. During CD measurement, DNA concentration was kept fixed and the concentrations of drugs were increased steadily. Each spectrum was recorded 10 min after drugs addition to ensure equilibration.

Isothermal titration calorimetry (ITC) measurements were performed in iTC200 microcalorimeter (Microcal-200) at 25^0C. All samples were degassed prior to use. The titration of G-quadruplex against drugs was performed by injecting drugs in 20 aliquot of 2 µL each with 200 seconds resting time between injections, into a solution with fixed concentration of GQ in the cell of 200 µL. The blank experiment was also performed by injecting drugs into PBS buffer and was used to correct dilution effect. The isotherm was analyzed using single-site binding model and fit by a nonlinear least squares fitting algorithm using the built-in Microcal LLC ITC software to yield the relevant thermodynamic parameter.

Melting study was performed using Varian Cary 300 Bio UV-Vis Spectrophotometer (Thermo Fisher Scientific, U.S.A.). Data were analyzed by using Origin-Pro 8 software. Thermal melting was monitored at 290 nm with heating rate 1^0C/min. Here we have provided melting temperatures (T_m) from best sigmoidal curve fit of the melting profile.

3. RESULTS AND DISCUSSION

3.1. Interaction of Proflavine with G-Quadruplex DNA:

3.1.a. Steady State Results of PF and GQ-DNA: Proflavine (PF) in buffer (PBS, pH 6.8) shows a single unstructured absorption band at ~444 nm (**Figure 8**) which is in good agreement with previous reports[21]. Increasing concentration of GQ-DNA results in heavily decreased in absorption (almost 53%) along with bathochromic shift from 444 nm to 457 nm up to maximum addition of GQ-DNA (13.5 μM). The strongly decreasing absorption peak might be an indication towards GQ-PF ground state complex formation whereas the huge shift (13 nm) in absorption position infers possible switch of polarity around PF molecules due to DNA binding interaction. The red shift infers that PF senses a less polar environment as it is well established that higher polarity around PF vicinity leads to strong blue shift of absorption[21]. The significant alteration of absorption spectra might be the first indication of interaction between PF and GQ-DNA.
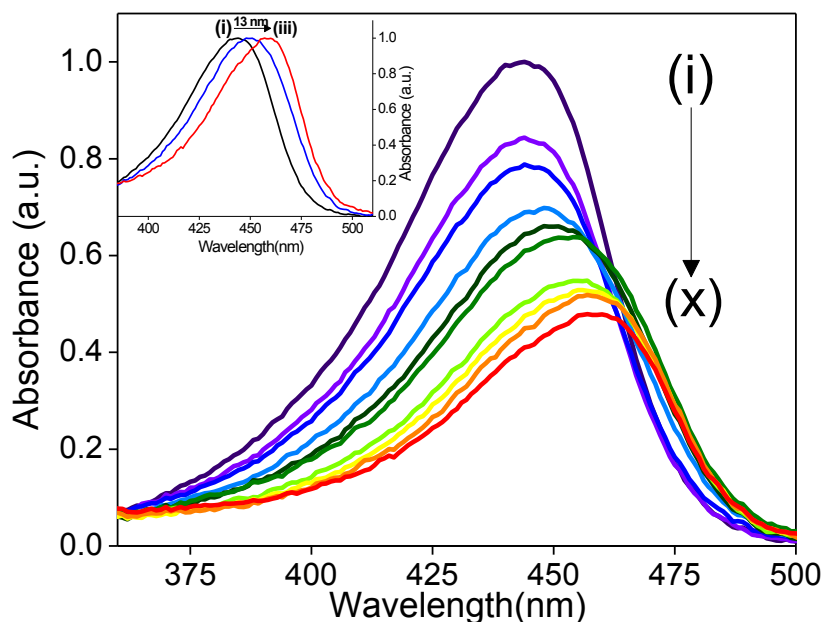

Figure 7. Absorption spectra of proflavine (4.5 μM) in potassium phosphate buffer (pH=6.8) containing 150 mM KCl with increasing concentration of [GQ-DNA]/ μM: (i) 0, (ii) 0.25, (iii) 0.5, (iv) 1.5, (v) 2.5, (vi) 3.5, (vii) 5, (viii) 7, (ix) 10, (x) 13.5 where inset shows stoke's shift with increasing concentration of [GQ-DNA]/ μM: (i) 0, (ii) 2.5, (iii) 13.5

The room-temperature emission spectra of PF in pH 6.8 show a single unstructured band with the emission maximum around 512 nm (**Figure 8A**). With the addition of GQ DNA, it exhibits a 4 nm blue shift (at highest GQ concentration, 13.5 µM) and, a severe quenching (80%) of fluorescence is observed up to maximum DNA concentration implying a strong interaction with GQ-DNA. Furthermore, there is almost 10-fold rise in steady state anisotropy value in presence of 13.5 µM GQ-DNA (**Figure 8B**). As anisotropy dictates the extent of rigidity offered by surrounding environment, a high anisotropy value concludes a strong binding interaction between PF and DNA.
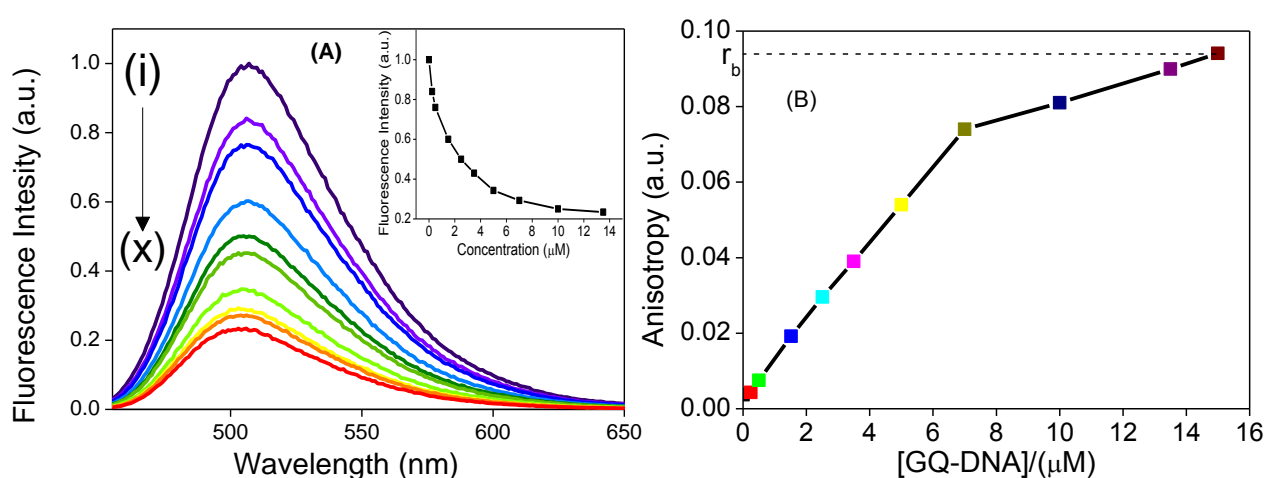
Figure 8: (A) Fluorescence spectra of proflavine (4.5 µM) in PBS (pH=6.8) with increasing GQ-DNA concentrations (in µM); where, i→x stands for 0, 0.25, 0.5, 1.5, 2.5, 3.5, 5, 7, 10, and 13.5. Inset shows intensity vs. [GQ-DNA] plot. (B) Steady state anisotropy of proflavine in the presence of varying concentration of G-quadruplex.

When we think about the reason of quenching two distinct possibilities comes in picture; either resonance energy transfer or electron transfer from nucleobases to PF. The possibility of resonance energy transfer can be easily ruled out since there is no overlap between the emission spectra of PF (donor) and the absorption spectrum of any of the nucleobases (acceptor). Hence probable reason for PF emission quenching is electron transfer between nucleobases and PF. Nucleobases (e.g. adenine (E_{ox}=1.5 eV)[31], cytidine (E_{ox} = 1.6eV) [31a], and guanosine (E_{ox} = 1.29 eV)[31a] thymidine (E_{ox} = 1.7 eV)[31b] act as potential electron donor to photoexcited proflavine ring (E_{ox} = -0.78V)[32]. We feel that positively charged PF molecules involves in electrostatic interaction with negatively charged phosphate backbone of GQ-DNA, and then PF interacts with DNA. A very similar view of PF intercalation in

wild DNA is recently reported by wilbee *et al* [33]. Note that, excited state electron transfer from nucleobases to PF leading to 80% quenching needs a very strong stacking interaction between molecules, which is possible either by intercalation between bases or by stacking at the top of the GQ strand. Although steady-state studies offer a glimpse of interaction between PF and GQ-DNA, it cannot give such explicit picture of the interaction, and hence, we have used time resolved emission, CD measurements, ITC and Job's plot (discussed later part of the thesis) to provide the molecular picture of interaction between PF and GQ-DNA.

The binding constant (K_b = 1.46×10^5 M^{-1}) is calculated from steady state anisotropy data using following equation 1[34] shown in Figure 9.

$$\frac{1}{f_b} = \frac{1}{K_b} \times \frac{1}{[GQ-DNA]} + 1 \qquad (1)$$

Where, f_b and K_b are bound fraction of PF and binding constant, respectively. To calculate bound fraction we used equation (2);[35]

$$f_b = \frac{r - r_f}{r_b - r_f} \qquad (2)$$

where, r, r_b and r_f are represent the anisotropy, anisotropy at saturation (see the Y-axis labelling in Figure 8 (B)) and free PF, respectively. The estimated binding constant is in good agreement with the observed binding affinity of alkaloids binding to GQ-DNA.[15a]
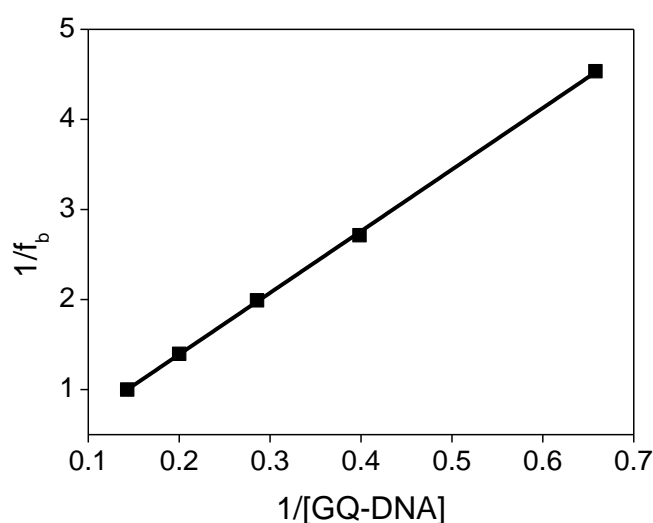
Figure 9. Binding isotherm plot using equation (1).

3.1.b Excited State Time-resolved Lifetime and Anisotropy Measurements:

Fluorescence lifetime measurement is an excellent technique to explore the excited-state environment around the fluorophores[35] and hence can contribute significantly to understand the PF-GQ-DNA interaction. In PBS buffer (pH 6.8) PF exhibits a single exponential decay having a lifetime component around 4.8 ns (**Figure 10, Table 1**), which is in close agreement to previous reports.[21] A comparison with previous works shows that irrespective to the polarity of the medium a 4.8 ns is ubiquitously present for PF decay, which might be attributed to the normal fluorescence lifetime of PF in water.
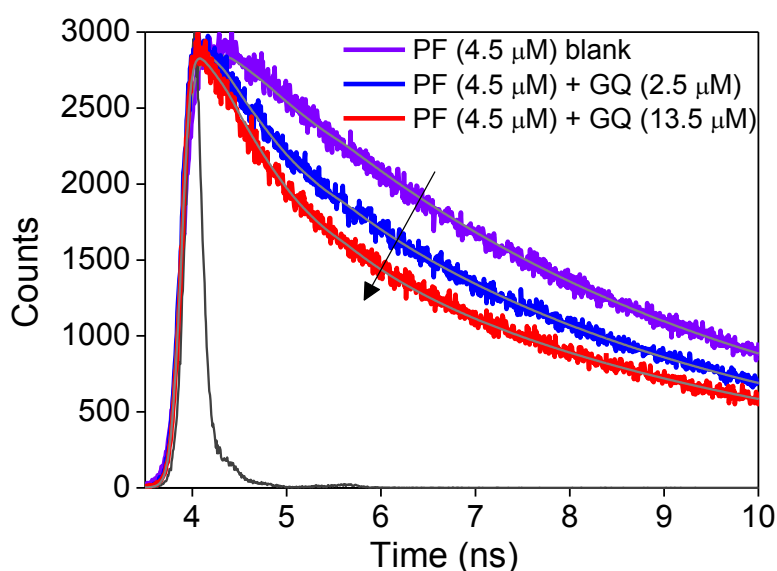
Figure 10: Time-resolved fluorescence decays of PF in buffer (pH=6.8) and in presence of different concentrations of GQ-DNA. Legends carry respective meaning.

Table 1: Time-resolved fluorescence decay parameters of PF in the absence and in presence of GQ-DNA, collected at 510 nm.

Sample	τ_1(ns)	τ_2 (ps)	a_1	a_2	τ_{av}* (ns)	$\chi2$
PF (4.5 μM) blank	4.80	-	1	-	4.8	1.04
PF(4.5 μM) + GQ (2.5 μM)	4.82	732	0.71	0.29	3.63	1.01
PF (4.5 μM) + GQ (13.5 μM)	5.1	841	0.56	0.44	3.22	1.09

*$\tau_{av} = \tau_1 a_1 + \tau_2 a_2$

With the gradual increase of GQ-DNA concentration, though the lifetime of the long component remains same a new shorter component of 800 ps starts appearing in the decay profile (**Table 1, Figure 10**). This reduced lifetime is an outcome of the quenching effect of PF by nucelobases. The respective contribution of short-lived component enhanced up to 45% till the maximum addition of GQ-DNA (~15 µM). This might infer the enhanced extent of complexation between PF and DNA at higher GQ concentration. The origin of the strong quenching in lifetime can be guessed to the base-stacking interaction between PF and GQ-DNA, which also corroborates well with the high extent of quenching in steady state experiment. Although our results predict that PF involves base stacking interaction with GQ-DNA, at this stage it will be difficult to get a clear insight about the location of PF molecules in GQ DNA.
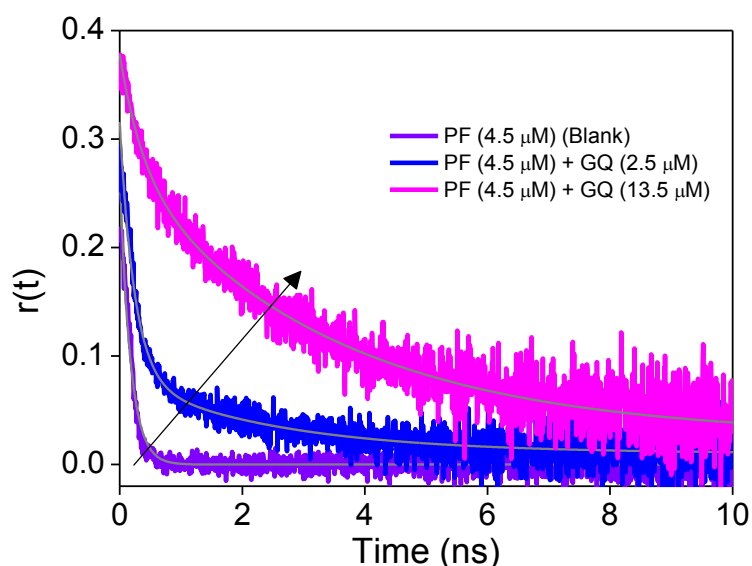
Figure 11: Time-resolved fluorescence anisotropy decays of PF in buffer (pH=6.8) and in presence of different concentration GQ-DNA. The legends carry respective meanings.

As polarization can give a vivid glance into the bound or unbound states of a molecule, this technique is employed to gather additional evidence in support of the interaction of the probe with native and DNA bound PF. Time-resolved fluorescence anisotropy is an efficient technique to measure the polarization of a molecule calculated using the following equation[35]

$$r(t) = \frac{I_{\parallel}(t) - GI_{\perp}(t)}{I_{\parallel}(t) + 2GI_{\perp}(t)} \qquad (3)$$

where, $I_\parallel(t)$ and $I_\perp(t)$ are fluorescence decays polarized parallel and perpendicular to the polarization of the excitation light, respectively. G is the correction factor for detector sensitivity to the polarization direction of the emission. Excited state anisotropy measurements infer about the rotational motion of the fluorophore, which directly reflects the extent of restriction imposed by the surrounding environment. When the probe binds to a DNA, the rotational motion of the probe is expected to be retarded and is reflected through

Table 2: Time-resolved anisotropy decay parameters of PF in the absence and in presence of GQ-DNA collected at 510 nm.

Sample	τ_{r1} (ns)	τ_{r2} (ns)	a_1	a_2	τ_{rav}* (ns)	χ^2
PF (4.5 µM) blank.	0.175	-	1	-	0.175	1.0704
PF(4.5 µM) + GQ (2.5 µM)	0.245	2.55	0.77	0.23	0.774	1.0190
PF(4.5 µM) + GQ (13.5 µM)	0.360	3.39	0.29	0.71	2.525	1.0842

*$\tau_{rav} = \tau_{r1}a_1 + \tau_{r2}a_2$

soaring rotational relaxation time of the probe. Time-resolved anisotropy results are presented in **Figure 11**. In the absence of DNA, the single exponential anisotropy decay is observed with rotational correlation time (τ_r) 175 ps. A single exponential rotational decay indicates that the probe molecules experience a homogeneous environment in normal buffer medium. In presence of GQ-DNA, the anisotropy decay is found to be multiexponential which might be an outcome of distinctly different rotational relaxation times from free and DNA-bound PF molecules. In presence of DNA a retarded component (3.4 ns) along with the ~175 ps component appears in the anisotropy decay profiles of PF. The fast anisotropy component represents the rotational time of unbound PF, whereas the long component represents the rotational motion of DNA bound PF. The estimated rotational relaxation times τ_r are used to determine the hydrodynamic volumes of inclusion complex formed between PF and GQ-DNA by using the following Stokes–Einstein relationship(4)[36].

$$\tau_r = \frac{1}{6D_r} = \frac{\eta V}{kT} \tag{4}$$

Where D_r and η are the rotational diffusion coefficient and viscosity of the medium, respectively, and V is the hydrodynamic molecular volume of the complex at absolute temperature T. We calculated the hydrodynamic radius of free and DNA bound PF. Interesting to note where free PF shows a hydrodynamic radius of 5.6 Å and the DNA bound PF shows a radius of ~15 Å. The increase in hydrodynamic radius is a confirmation of GQ-DNA-PF non-covalent complex formation.

3.1.c. Circular Dichroism (CD) and Thermal Melting (TM) Measurements; a Structural Glimpse of PF, GQ-DNA Interaction:

Circular dichroism (CD) is a very sensitive technique to explore the modification of the secondary structure of biopolymers as a result of interaction with small molecules[37]. Therefore we have exploited the CD technique in order to examine proflavine-induced structural alteration of G-quadruplex. In this study GQ-DNA concentration was kept constant (5 µM) throughout the measurements and changes of CD spectra were monitored with increasing concentrations of drug (PF). The CD spectra of GQ-DNA exhibits peak at ~288 nm and shoulder at ~270, which are characteristics features of anti-parallel and parallel DNA, respectively (**Figure. 12**).
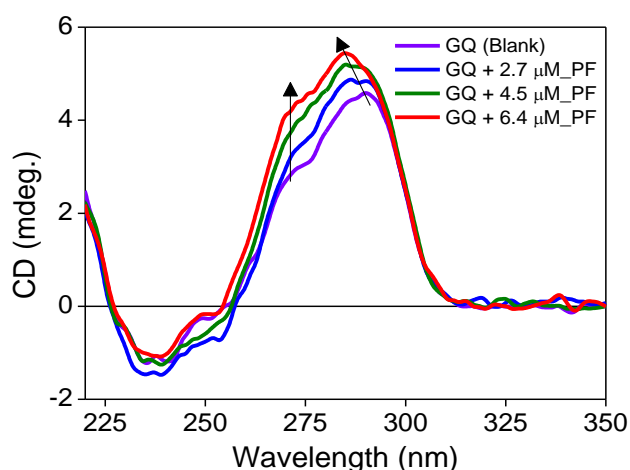

Figure 12. CD spectra of GQ-DNA (5µM) at different concentration of PF, where legends carry the respective meaning.

The above mentioned feature confirmed the hybrid (3+1) G-quadruplex (in which three strands are oriented in one direction and the fourth is in the opposite direction) structure formation and is consistent with previously reported in literature for similar

sequences in presence of K^+.[38] Enhancement in CD signal with the gradual addition of PF indicates the stabilization of G-quadruplex. Moreover, the CD signal at ~288 nm is shifting towards the lower wavelength and the shoulder at ~270 nm becomes more prominent in presence of PF. This CD signal infers the PF binding to GQ-DNA leading more towards parallel G-quadruplex structure as the 270 nm peak is characteristic to a parallel GQ-DNA.

To confirm the stability effect by proflavine binding to DNA we have carried out thermal melting study for free and PF bound DNA. Thermal melting profiles of GQ-DNA and PF bound GQ-DNA is shown in **Figure 13**. Binding of proflavine to GQ-DNA offers a $8(\pm 0.5)^o$C increase in melting temperature, which infers stabilization of GQ-DNA due to proflavine binding. It has been earlier reported that Ethidium derivatives binding to GQ-DNA increasing in melting temperature between 7 to 10 ^{0}C inhibits the telomerase activity with high affinity (IC_{50} in nM)[39]. Therefore, considering 8^0C increase in melting temperature, it is reasonable to assume that proflavine can also act as a telomerase inhibitor.

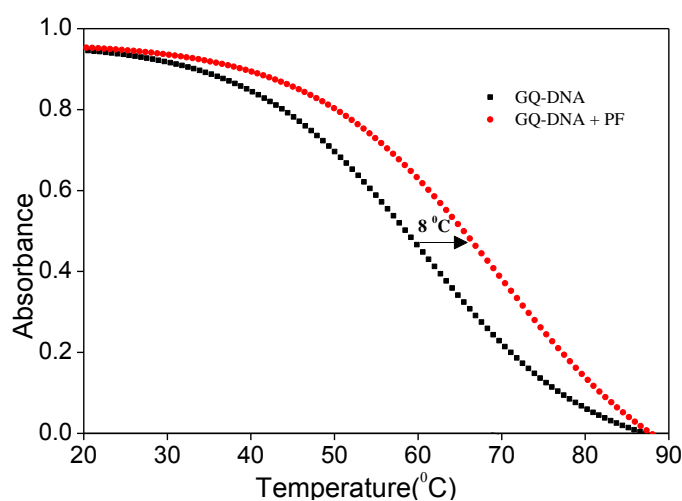**Figure 13.** Melting curve for GQ-DNA in absence and in presence of proflavine (PF).

3.1.d. Isothermal Titration Calorimetry (ITC): Thermodynamics of Binding

To obtain thermodynamic parameters of proflavine binding with GQ-DNA, isothermal titration calorimetry (ITC) was performed. It is an effective and sensitive tool to characterize binding of small molecules to biomacromolecules and might

provide valuable key insights into molecular forces that drive the complex formation, number of binding site and binding energies[40]. Isothermal titration calorimetric profiles for proflavine with GQ-DNA are shown in **Figure 14**. Each peak of the binding isotherm in the upper panels represents each of the PF injections. The amount of heat liberated by successive addition of PF is plotted against the molar ratio of PF to GQ-DNA in the lower panels. A standard nonlinear least-squares regression binding model for one-site binding is employed to fit the data. The best fit is shown in the lower panel. Thermodynamic parameter extracted from the fitting of binding curves are summarised in **Table 3**. From this study it is revealed that binding is enthalpically as well as entropically driven phenomenon with a high change of free energy (ΔG) -8.24 kcal/mol having binding affinity (K) of 1.13×10^6 M^{-1}. The positive entropy change may originate mainly from two potential sources. Firstly, it may be attributed to the increased in solvent entropy because of binding of PF releases water molecules. Secondly, the increased entropy may be appearing due to increase in mobility of the adenine residues in the edgewise loops. It has been shown earlier that when a planner aromatic compounds interact with (3+1) hybrid G-quadruplex by end stacking, results in an increased mobility of adenine residues in edgewise loops (**Scheme 1**)[41]. The proflavine binding-induces destacking of these bases leads to increase in the configurational entropy of GQ-DNA.
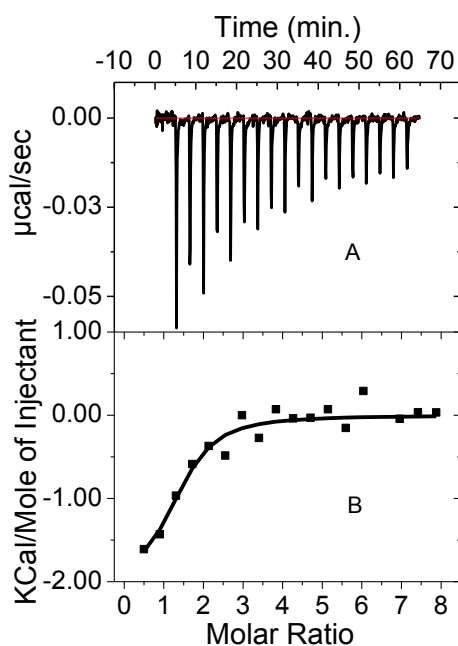

Figure 14. Upper panel (A) shows raw data for the titration of GQ-DNA (in cell) with proflavine (in syringe), where as the lower panel (B) shows integrated heat profile of the calorimetric titration shown in panel (A). The solid line represents the best nonlinear least-square fit to a single binding site model.

Table 3. Thermodynamic Parameters from Isothermal Titration Calorimetry (ITC) data.

Binding constant (K) (M^{-1})	N	ΔH $(kcal.mol^{-1})$	ΔS $(cal.mol^{-1}K^{-1})$	ΔG $(kcal.mol^{-1})$
$(1.13 \pm 0.65) \times 10^{6}$	1.37 ± 0.18	-2.042 ± 0.37	20.8	-8.24

Interestingly, from ITC number of binding sites are found to be nearly 1.5, which further supports the binding stoichiomety (GQ-DNA:PF = 2:3) determined from the break point in the Job's plot[42] (using fluorescence intensities at different molar ratios of PF (**Figure 15**).
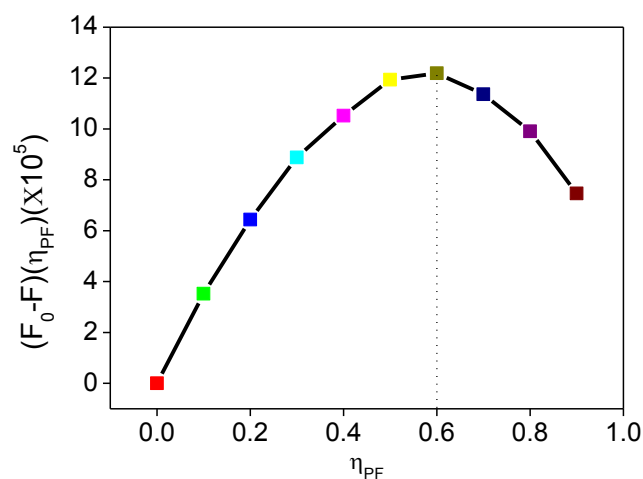
Figure 15: Job's plot of PF with GQ-DNA interaction. Here η_{PF} represents mole fraction of proflavine (PF)

Literature reports of binding stoichiometries for the small molecules interaction with G-quadruplex are highly diverse. Planar aromatic compounds are known to bind with GQ-DNA via external end π-π stacking to the surface of the G-quartet at the one or both of ends[15b, 41]. Molecules like porphyrins[43], phenanthroline derivatives[44], plant alkaloids (Berberine and Sanguinarine)[45], Quindoline and its, isaindigotone derivatives[46], etc show multiple binding modes with GQ-DNA. Whereas Ellipticine binding was found to be 3:2 (Ellipticine:H24)[38a] Combining all these previous reports along with the observed binding stoichiometry (PF:GQ-DNA = 3:2) from ITC and job's plot, we propose that one molecule of proflavine (PF) gets sandwiched between two molecules of GQ-DNA. Moreover, two proflavine

molecules are bound (end stacked) to the two remaining ends of GQ-DNA (**Scheme 2**).
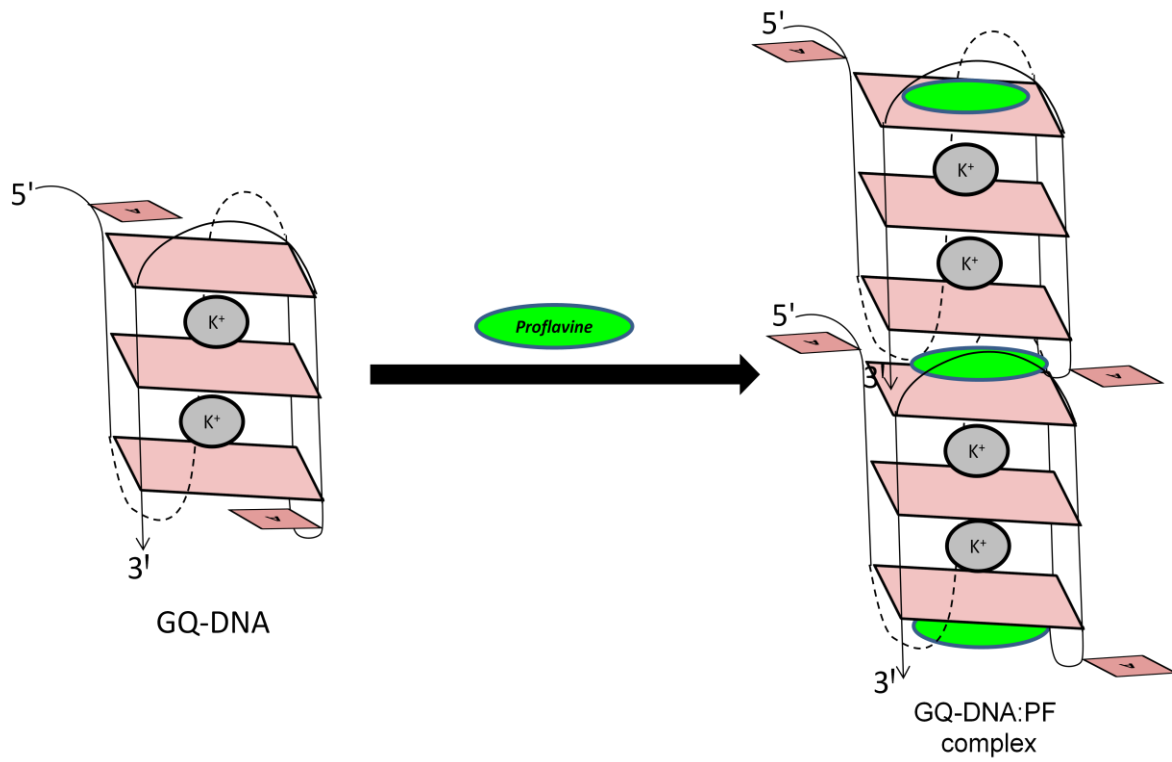
Scheme 2. Proposed molecular picture of binding interaction between PF and (3+1) hybrid telomeric GQ-DNA.

3.2. Interaction of Harmine with G-Quadruplex

3.2.a. Steady-State Absorption and Emission Results:
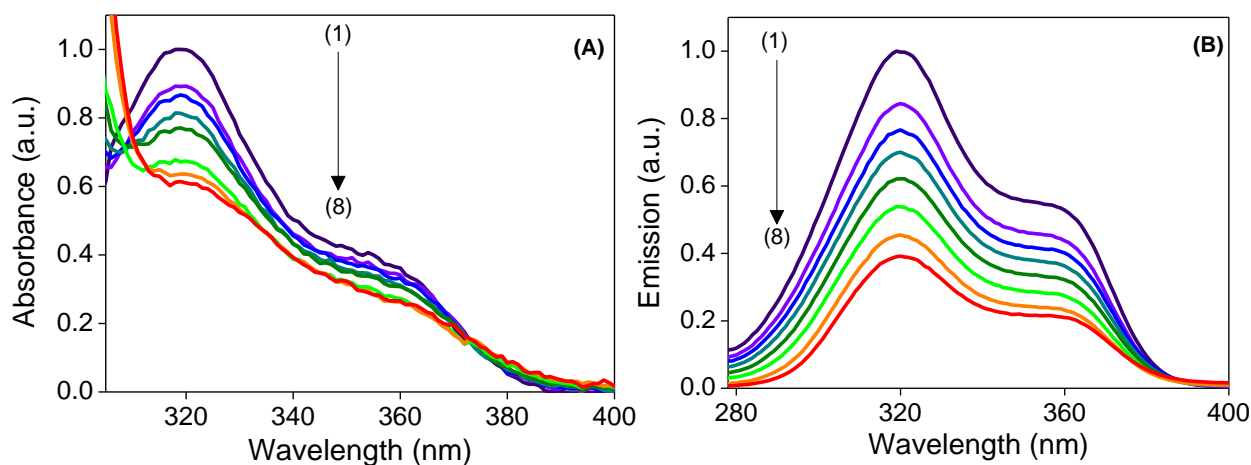
Figure 16. Absorption spectra (A), and excitation spectra (B) of harmine (4.4µM) in potassium phosphate buffer (pH=6.8) containing 150 mM KCl with increasing concentration of [GQ-DNA]/ µM: (1) 0, (2) 0.32, (3) 0.129, (4) 2.55, (5) 4.4, (6) 6.78, (7) 11.82, (8) 17.

Absorption spectra of harmine in presence of different concentration of GQ-DNA are shown in **Figure 16**. The absorbance is exclusively coming from the cationic form of the drug, because all the measurements were carried out in PBS of pH = 6.8 and it is known that the protonation pK_a of hamine is 7.8[30]. The absorption band in between 280 and 400 nm are mainly coming from the π-π* transition[29]. Upon addition of GQ-DNA, absorption profiles show a significant decrement. These noteworthy changes in absorption features provide preliminary notion about strong binding interactions between protonated harmine and G-quadruplex in the ground state. We have further employed steady state and time resolved emission measurements to divulge specific details of the interaction, and will be discussed afterwards

At the room-temperature emission spectra of harmine in pH 6.8 show a single unstructured band with the emission maximum around 420 nm (**Figure 17**) which is exclusively from cationic form of harmine. With the successive addition of GQ-DNA, emission spectra exhibit a severe quenching, and at maximum DNA concentration the fluorescence is quenched ~65% of its original intensity.
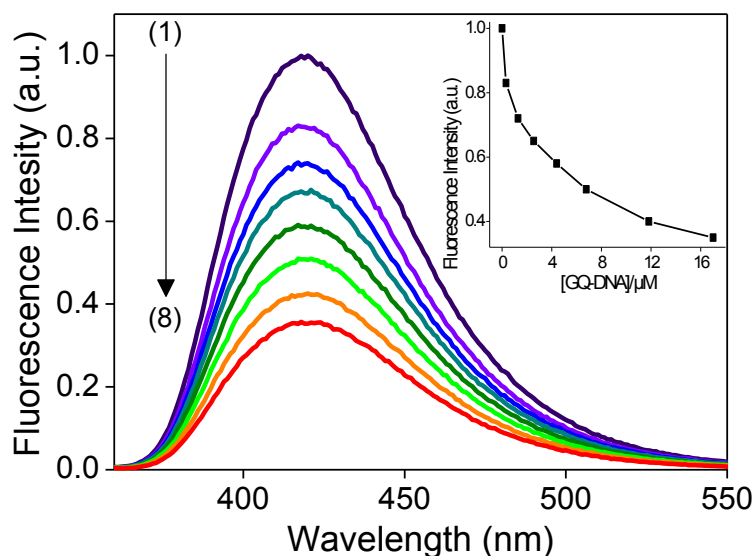
Figure 17. Fluorescence spectra of harmine (4.4 µM) in potassium phosphate buffer (pH=6.8) containing 150 mM KCl with increasing concentration of [GQ-DNA]/µM: (1) 0, (2) 0.32, (3) 0.129, (4) 2.55, (5) 4.4, (6) 6.78, (7) 11.82, (8) 17.

This implies a strong interaction of the drug with GQ-DNA. When we think about the possible reasons of quenching, two distinct possibilities comes into the picture; either resonance energy transfer or electron transfer from nucleobases to harmine. The possibility of resonance energy transfer can be easily ruled out, since there is no overlap between the emission spectra of harmine (donor) and the absorption spectrum of any of the four nucleobases (acceptor).). Hence probable reason for PF emission quenching is electron transfer between nucleobases and PF. Nucleobases (e.g. adenine (E_{ox}=1.5 eV)[31], cytidine (E_{ox} = 1.6eV) [31a], and guanosine (E_{ox} = 1.29 eV)[31a] thymidine (E_{ox} = 1.7 eV)[31b]) act as potential electron donor to photoexcited harmine ring acts as an acceptor (E_{ox} = 0.3 eV)[47]. We anticipate that the cationic form of the drug is attracted by the phosphate backbone of GQ-DNA and binds to the DNA. After that electron transfer from nucleobases to harmine takes place and leads to severe quenching. A very similar view of harmine intercalation in calf thymus DNA is reported by Guy Duportail and Hans Lami[19a] Note that, excited state electron transfer from nucleobase(s) to harmine leading to 65% quenching needs a very strong stacking interaction between molecules, which is possible either by intercalation between bases or by stacking at the top or bottom of the GQ strand. Although steady-state studies offer a glimpse of interaction between harmine and GQ-DNA, it cannot provide such explicit picture of the interaction, hence we have to

use other techniques like, time resolved emission, CD measurements, ITC measurements and Job's plot, which will be discussed hereafter.

3.2.b. Excited State Time-resolved Emission and Anisotropy Measurements:

Fluorescence lifetime measurement is an excellent technique to explore the excited-state environment around the fluorophores and hence can contribute significantly to understand the harmine-GQ-DNA interaction. InPBS (pH 6.8) harmine exhibits a single exponential decay having a lifetime component around 6.6 ns (**Figure 18, Table 4**), which is in close agreement to previous reports.[29-30] With the gradual increase of GQ-DNA concentration, though the lifetime of the long component (6.6) remains same a new shorter component of 1.2 ns starts appearing (**Table 4**) in the decay profile. The contribution of short-lived component enhanced up to 33% till the addition of maximum concentration of GQ-DNA (~17 µM).The reduced lifetime is a definitely outcome of the quenching effect of harmine by nucelobases.

The origin of the quenched lifetime can be guessed to the base-stacking interaction between harmine and GQ-DNA, which corroborates well with the high extent of quenching in steady state spectra.
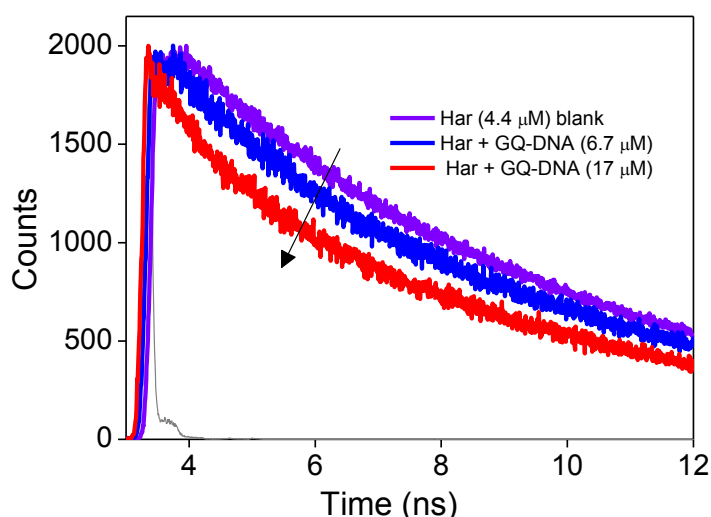

Figure 18: Time-resolved fluorescence decays of harmine in buffer (pH=6.8) and in presence of different concentrations of GQ-DNA. Legends carry respective meaning.

Table 4. Fluorescence decay parameters of harmine (4.37 μM) in absence and presence of GQ-DNA collected at 420 nm.

[GQ-DNA]/μM	τ_1 (ns)	τ_2 (ns)	a_1	a_2	τ_{av}^* (ns)	χ^2
0	6.55	-	1	-	6.55	1.06
4.4	6.68	1.08	0.86	0.14	5.92	1.05
6.78	6.71	1.28	0.83	0.17	5.82	1.01
11.82	6.80	1.04	0.73	0.27	5.23	1.07
17	6.81	1.01	0.67	0.33	4.92	1.10

$^*\tau_{av} = \tau_1 a_1 + \tau_2 a_2$

Excited state anisotropy measurements infer about the rotational motion of the fluorophore, which directly reflects the extent of restriction imposed by the surrounding environment. When the probe binds to a DNA, the rotational motion of the probe is expected to be retarded and is reflected through soaring rotational relaxation time of the probe. Time-resolved anisotropy results are presented in **Figure 19**. In the absence of DNA, the single exponential anisotropy decay is observed with rotational correlation time($\tau_{r)}$ 146 ps. A single exponential rotational decay indicates that the probe molecules experience a homogeneous environment in normal buffer medium. In presence of GQ-DNA, the anisotropy decay is found to be multi-exponential which might be an outcome of distinctly different rotational relaxation times from free and DNA-bound harmine molecules. In presence of DNA a retarded component (2 ns) along with the ~146 ps component appears in the anisotropy decay profiles of harmine. The fast anisotropy component represents the rotational time of unbound harmine, whereas the long component represents the rotational motion of DNA bound harmine. The estimated rotational relaxation times τ_r are used to determine the hydrodynamic radius of inclusion complex formed between harmine and GQ-DNA by using Stokes–Einstein relationship[36] (equation 3).

Interesting to note, the DNA bound harmine shows a radius ~12.6 Å, where free harmine shows a hydrodynamic radius 5.3 Å. The significant increase in hydrodynamic radius is a proof for the non-covalent GQ-DNA-harmine complex formation, which supports our conjecture that harmine involves in stacking interaction either intercalation between bases or by stacking at the top or bottom of the GQ strand.
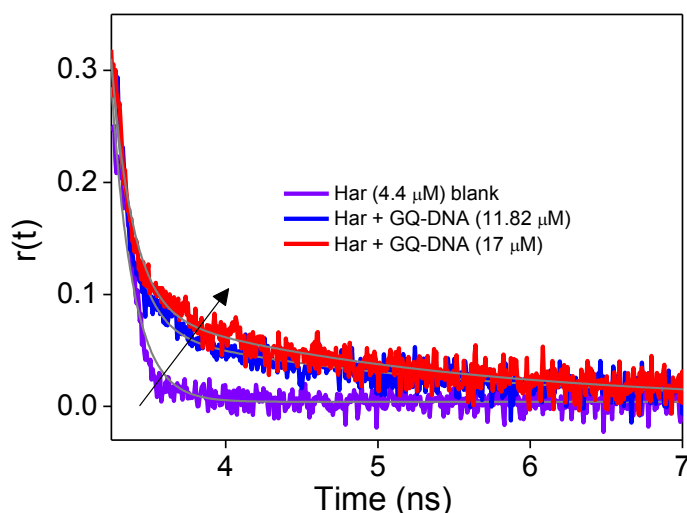
Figure 19: Time-resolved anisotropy decays of harmine in buffer (pH=6.8) and in presence of different concentrations of GQ-DNA. Legends carry respective meaning.

Table 5. Anisotropy decay parameters of harmine (4.37 µM) in absence and presence of GQ-DNA collected at 420 nm.

[GQ-DNA]/µM	τ_{r1} (ps)	τ_{r2} (ps)	a_1	a_2	τ_{rav}* (ps)	χ^2
0	146	-	1	-	146	1.05
11.82	142	2000	0.83	0.17	462	1.07
17	146	2000	0.79	0.21	553	1.01

*$\tau_{rav} = \tau_{r1}a_1 + \tau_{r2}a_2$

3.2.c. Cicular Dichroism (CD); a Structural Glimpse of Harmine, GQ-DNA Interaction:

Circular dichroism (CD) is a very sensitive technique to explore the modification of the secondary structure of biopolymers as a result of interaction with small molecules[37]. Therefore we have exploited the CD technique in order to examine

proflavine-induced structural alteration of G-quadruplex. In this study GQ-DNA concentration was kept constant (8 µM) throughout the measurements and changes of CD spectra were monitored with increasing concentrations of harmine. The CD spectra of GQ-DNA exhibits peak at ~288 nm and shoulder at ~270, which are characteristics features of anti-parallel and parallel DNA, respectively (**Figure 20**). This confirmed hybrid (3+1) G-quadruplex (in which three strands are oriented in one direction and the fourth is in the opposite direction) formation are consistent with previously reported in literature for similar sequences in presence of K^+.[38]

Though CD is a very sensitive technique for examining the structural change in G-quadruplex due to drug interaction, but it pose an unique problem when drug itself shows huge CD signal in the same region of G-quadruplex. Herein, we tried to do CD experiment in order to examine harmine-induced structural alteration of G-quadruplex, but we didn't get any pattern in CD signal because harmine itself shows a huge CD signal in the same region of G-quadruplex(200 nm to 350 nm) shown in **Figure 20**.
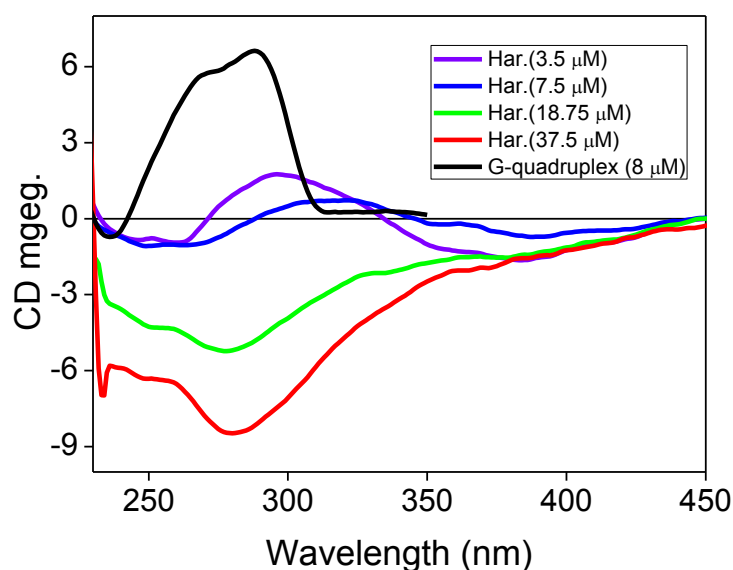
Figure 20. CD spectra for for G-qudruplex (8µM) and harmine at different concentration, where legends carry the respective meaning.

We also had plan to do isothermal titration calorimetry (ITC) study to get insight into the thermodynamic parameters, which may provide valuable key insights into molecular forces that drive the complex formation, and also number of binding site and binding energies. But we could not carry out due to instrument (ITC) malfunctions since last one month. In future, we can provide more information about

harmine-G-DNA interaction, as soon as instrument starts functioning. We are also planning to do thermal melting study to explore the stability of GQ-DNA achieved by the binding of harmine. All the above mentioned studies are required in order to predict precisely the binding feature of GQ-DNA and harmine. Although in absence of the above mentioned studies it is hard to predict the binding characteristic, we have tried to find out the stoichiometry of binding between harmine and GQ-DNA with the help of Job's plot. The break point in the Job's plot (using fluorescence intensities at different molar ratios of harmine)[42] (**Figure 21**), indicates the 2:3 binding stoichiometry (GQ-DNA:Harmine) of the complex. Therefore, based on the Job's plot and other experimental evidences we propose that one harmine is stacked in between two quartets of the DNA where each of the other open side of GQ-DNA contained a stacked harmine (**Scheme 3**).
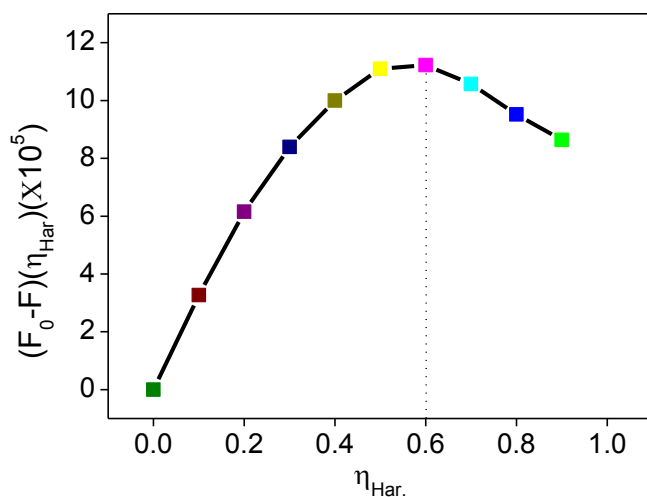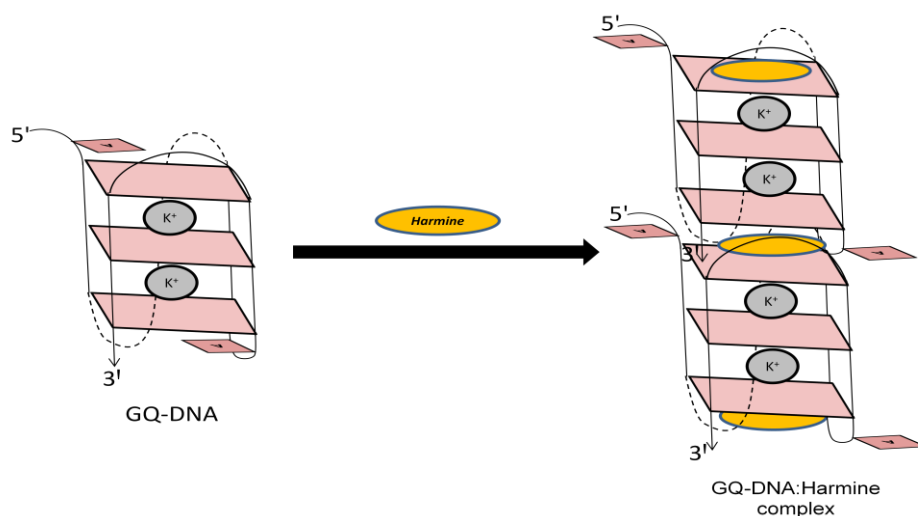

Figure 21. Job's plot of harmine with GQ-DNA. Here η_{Har} represents mole fraction of harmine.

Scheme 3. Proposed molecular picture of binding Interaction between harmine and (3+1) hybrid telomeric GQ-DNA.

4. <u>CONCLUSIONS</u>:

In this thesis, we have shown that proflavine binds to human telomeric GQ-DNA with high binding affinity ($K_b = 1 \times 10^6$ M^{-1}). Binding is entalpically as well as entropycally driven phenomenon with a 3:2 (PF:GQ-DNA) stoichiometry. Moreover, PF binding to GQ-DNA induces G-quadruplex structure more towards parallel structure. Furthermore, GQ-DNA complexed with PF is stabilized and it is reflected by increased melting temperature (~8 ^{o}C). With the observed binding stoichiometry (PF:GQ-DNA = 3:2) from ITC and job's plot, we propose that one molecule of proflavine (PF) gets sandwiched between two molecules of GQ-DNA. Moreover, two proflavine molecules are bound (end stacked) to each of the two remaining ends of GQ-DNA.

Study of interaction between harmine and G-quadruplex depicts a noteworthy decrease in absorption and severe quenching in fluorescence intensity upon addition of GQ-DNA and is an indication of a strong stacking interaction between harmine and G-quadruplex. The stacking interaction is further supported by excited state time-resolved studies, where it is found that hydrodynamic radius increased significantly in harmine bound GQ-DNA. From job's plot, we got 3:2 (Harmine:GQ-DNA) binding stoichiometry, which suggests that one harmine molecule resides in between two molecules of GQ-DNA, and two other harmine molecules are bound (end stacked) to each of the two remaining ends of GQ-DNA. The confirmed molecular picture and thermodynamic parameters of interaction between harmine and GQ-DNA will be provided by ITC study, which will be performed in near future.

REFRENCES:

1. (a) Kaur, H.; Babu, B. R.; Maiti, S., Perspectives on Chemistry and Therapeutic Applications of Locked Nucleic Acid (LNA). *Chem. Rev.* **2007,** *107* (11), 4672-4697; (b) Jung, Y.; Lippard, S. J., Direct Cellular Responses to Platinum-Induced DNA Damage. *Chem. Rev.* **2007,** *107* (5), 1387-1407; (c) Stubbe, J.; Kozarich, J. W., Mechanisms of bleomycin-induced DNA degradation. *Chem. Rev.* **1987,** *87* (5), 1107-1136; (d) Sherman, S. E.; Lippard, S. J., Structural aspects of platinum anticancer drug interactions with DNA. *Chem. Rev.* **1987,** *87* (5), 1153-1181; (e) Gill, M. R.; Thomas, J. A., Ruthenium(ii) polypyridyl complexes and DNA-from structural probes to cellular imaging and therapeutics. *Chem. Soc. Rev.* **2012,** *41* (8), 3179-3192.

2. (a) Doluca, O.; Withers, J. M.; Filichev, V. V., Molecular Engineering of Guanine-Rich Sequences: Z-DNA, DNA Triplexes, and G-Quadruplexes. *Chem. Rev.* **2013,** *113* (5), 3044-3083; (b) Xu, Y., Chemistry in human telomere biology: structure, function and targeting of telomere DNA/RNA. *Chem. Soc. Rev.* **2011,** *40* (5), 2719-2740; (c) Murat, P.; Singh, Y.; Defrancq, E., Methods for investigating G-quadruplex DNA/ligand interactions. *Chem. Soc. Rev.* **2011,** *40* (11), 5293-5307; (d) Collie, G. W.; Parkinson, G. N., The application of DNA and RNA G-quadruplexes to therapeutic medicines. *Chem. Soc. Rev.* **2011,** *40* (12), 5867-5892.

3. Gellert, I.; Lipsett, M. N.; Davies, D. R., Helix formation by guanylic acid. *Proc. Natl. Acad. Sci. U.S.A.* **1962,** *48*, 2013-2018.

4. Yaku, H.; Fujimoto, T.; Murashima, T.; Miyoshi, D.; Sugimoto, N., Phthalocyanines: a new class of G-quadruplex-ligands with many potential applications. *Chem. Commun.* **2012,** *48* (50), 6203-6216.

5. (a) Henderson, E.; Hardin, C. C.; Walk, S. K.; Tinoco Jr, I.; Blackburn, E. H., Telomeric DNA oligonucleotides form novel intramolecular structures containing guanine·guanine base pairs. *Cell* **1987,** *51* (6), 899-908; (b) Phan, A. T.; Modi, Y. S.; Patel, D. J., Propeller-Type Parallel-Stranded G-Quadruplexes in the Human c-myc Promoter. *J. Am. Chem. Soc.* **2004,** *126* (28), 8710-8716; (c) Siddiqui-Jain, A.; Grand, C. L.; Bearss, D. J.; Hurley, L. H., Direct evidence for a G-quadruplex in a promoter region and its targeting with a small molecule to repress c-MYC

transcription. *Proc. Natl. Acad. Sci. USA* **2002,** *99* (18), 11593-11598; (d) Todd, A. K.; Haider, S. M.; Parkinson, G. N.; Neidle, S., Sequence occurrence and structural uniqueness of a G-quadruplex in the human c-kit promoter. *Nucleic Acids Res.* **2007,** *35* (17), 5799-5808; (e) Shirude, P. S.; Okumus, B.; Ying, L.; Ha, T.; Balasubramanian, S., Single-Molecule Conformational Analysis of G-Quadruplex Formation in the Promoter DNA Duplex of the Proto-Oncogene C-Kit. *J. Am. Chem. Soc.* **2007,** *129* (24), 7484-7485.

6. (a) Lim, K. W.; Amrane, S.; Bouaziz, S.; Xu, W.; Mu, Y.; Patel, D. J.; Luu, K. N.; Phan, A. T., Structure of the Human Telomere in K+ Solution: A Stable Basket-Type G-Quadruplex with Only Two G-Tetrad Layers. *J. Am. Chem. Soc.* **2009,** *131* (12), 4301-4309; (b) Parkinson, G. N.; Lee, M. P. H.; Neidle, S., Crystal structure of parallel quadruplexes from human telomeric DNA. *Nature* **2002,** *417* (6891), 876-880.

7. (a) Bhasikuttan, A. C.; Mohanty, J.; Pal, H., Interaction of Malachite Green with Guanine-Rich Single-Stranded DNA: Preferential Binding to a G-Quadruplex. *Angew. Chem. Int. Ed.* **2007,** *46* (48), 9305-9307; (b) Rezler, E. M.; Seenisamy, J.; Bashyam, S.; Kim, M.-Y.; White, E.; Wilson, W. D.; Hurley, L. H., Telomestatin and Diseleno Sapphyrin Bind Selectively to Two Different Forms of the Human Telomeric G-Quadruplex Structure. *J. Am. Chem. Soc.* **2005,** *127* (26), 9439-9447.

8. Dahse, R.; Fiedler, W.; Ernst, G., Telomeres and telomerase: biological and clinical importance. *Clin. Chem.* **1997,** *43* (5), 708-714.

9. Lingner, J.; Cooper, J. P.; Cech, T. R., Telomerase and DNA end replication: no longer a lagging strand problem? *Science* **1995,** *269* (5230), 1533-1534.

10. (a) Harley, C. B.; Futcher, A. B.; Greider, C. W., Telomeres shorten during ageing of human fibroblasts. *Nature* **1990,** *345* (6274), 458-460 ; (b) Nakamura, K.-I.; Izumiyama-Shimomura, N.; Sawabe, M.; Arai, T.; Aoyagi, Y.; Fujiwara, M.; Tsuchiya, E.; Kobayashi, Y.; Kato, M.; Oshimura, M.; Sasajima, K.; Nakachi, K.; Takubo, K., Comparative Analysis of Telomere Lengths and Erosion with Age in Human Epidermis and Lingual Epithelium. *J. Invest. Derm.* **2002,** *119* (5), 1014- 1019.

11. Greider, C. W.; Blackburn, E. H., Identification of a specific telomere terminal transferase activity in tetrahymena extracts. *Cell* **1985,** *43* (2, Part 1), 405-413.

12. Freeman, S., *Biological Science*. 2 ed.; Pearson Prentice Hall: New Jersey, U.S.A, 2005.

13. (a) Greider, C. W.; Blackburn, E. H., Identification of a specific telomere terminal transferase activity in tetrahymena extracts. *Cell* **1985,** *43* (2), 405-413; (b) Morin, G. B., The human telomere terminal transferase enzyme is a ribonucleoprotein that synthesizes TTAGGG repeats. *Cell* **1989,** *59* (3), 521-529; (c) Kim, N.; Piatyszek, M.; Prowse, K.; Harley, C.; West, M.; Ho, P.; Coviello, G.; Wright, W.; Weinrich, S.; Shay, J., Specific association of human telomerase activity with immortal cell and cancer. *Science* **1994,** *266*, 2011-2015.

14. Huppert, J. L.; Balasubramanian, S., G-quadruplexes in promoters throughout the human genome. *Nucleic Acids Res.* **2007,** *35* (2), 406-413.

15. (a) Bessi, I.; Bazzicalupi, C.; Richter, C.; Jonker, H. R. A.; Saxena, K.; Sissi, C.; Chioccioli, M.; Bianco, S.; Bilia, A. R.; Schwalbe, H.; Gratteri, P., Spectroscopic, Molecular Modeling, and NMR-Spectroscopic Investigation of the Binding Mode of the Natural Alkaloids Berberine and Sanguinarine to Human Telomeric G-Quadruplex DNA. *ACS Chem. Biol.* **2012,** *7* (6), 1109-1119; (b) Xue, L.; Ranjan, N.; Arya, D. P., Synthesis and Spectroscopic Studies of the Aminoglycoside (Neomycin)−Perylene Conjugate Binding to Human Telomeric DNA. *Biochemistry* **2011,** *50* (14), 2838-2849; (c) Chung, W. J.; Heddi, B.; Tera, M.; Iida, K.; Nagasawa, K.; Phan, A. T., Solution Structure of an Intramolecular (3 + 1) Human Telomeric G-Quadruplex Bound to a Telomestatin Derivative. *J. Am. Chem. Soc.* **2013,** *135* (36), 13495-13501; (d) Zahler, A. M.; Williamson, J. R.; Cech, T. R.; Prescott, D. M., Inhibition of telomerase by G-quartet DMA structures. *Nature* **1991,** *350* (6320), 718-720; (e) Sun, D.; Thompson, B.; Cathers, B. E.; Salazar, M.; Kerwin, S. M.; Trent, J. O.; Jenkins, T. C.; Neidle, S.; Hurley, L. H., Inhibition of Human Telomerase by a G-Quadruplex-Interactive Compound. *J. Med.Chem.* **1997,** *40* (14), 2113-2116; (f) Clark, G. R.; Pytel, P. D.; Squire, C. J.; Neidle, S., Structure of the First Parallel DNA Quadruplex-Drug Complex. *J. Am. Chem. Soc.* **2003,** *125* (14), 4066-4067.

16. Sarkar, D.; Das, P.; Basak, S.; Chattopadhyay, N., Binding Interaction of Cationic Phenazinium Dyes with Calf Thymus DNA: A Comparative Study. *J. Phys. Chem. B* **2008,** *112* (30), 9243-9249.

17. (a) Denny, W. A., Acridine derivatives as chemotherapeutic agents. *Curr. Med. Chem.* **2002,** *9* (18), 1655-65; (b) P1, B.; J, B.; T, G.; M., T., Acridine and acridone derivatives, anticancer properties and synthetic methods: where are we now? *Anticancer Agents Med. Chem.* **2007,** *7* (2), 139-169.

18. Li, S.; Cooper, V. R.; Thonhauser, T.; Lundqvist, B. I.; Langreth, D. C., Stacking Interactions and DNA Intercalation. *J. Phys. Chem. B* **2009,** *113* (32), 11166-11172.

19. (a) Kingsbury, W. D.; Boehm, J. C.; Jakas, D. R.; Holden, K. G.; Hecht, S. M.; Gallagher, G.; Caranfa, M. J.; McCabe, F. L.; Faucette, L. F.; Johnson, R. K.; Hertzberg, R. P., Synthesis of water-soluble (aminoalkyl)camptothecin analogs: inhibition of topoisomerase I and antitumor activity. *J. Med.Chem.* **1991,** *34* (1), 98-107; (b) Pommier; Yves, Topoisomerase I inhibitors: camptothecins and beyond. *Nature* **2006,** *6* (10), 789-802.

20. Waring, M. J., DNA Modification and Cancer. *Annu. Rev. Biochem.* **1981,** *50* (1), 159-192.

21. Kumar, K. S.; Selvaraju, C.; Malar, E. J. P.; Natarajan, P., Existence of a New Emitting Singlet State of Proflavine: Femtosecond Dynamics of the Excited State Processes and Quantum Chemical Studies in Different Solvents. *J. Phys. Chem. A* **2011,** *116* (1), 37-45.

22. Diverdi, L. A.; Topp, M. R., Subnanosecond time-resolved fluorescence of acridine in solution. *J. Phys. Chem.* **1984,** *88* (16), 3447-3451.

23. Chopra; N., R.; Nayar; L., S.; Chopra; C., I., Glossary of Indian

Medicinal Plants. *Council of Scientific and Industrial Research: New Delhi* **1956**, 187.

24. (a) Shoemaker, D. W.; Bidder, T. G.; Boettger, H. G.; Cummins, J. T.; Evans, M., Combined gas chromatography and mass spectrometry of aromatic β-carbolines. *J. Chromatogr. A* **1979,** *174* (1), 159-164; (b) McKenna, D. J.; Towers, G. H. N., Ultra-violet mediated cytotoxic activity of β-carboline alkaloids. *Phytochemistry* **1981,** *20* (5), 1001-1004.

25. Nafisi, S.; Bonsaii, M.; Maali, P.; Khalilzadeh, M. A.; Manouchehri, F., β-Carboline alkaloids bind DNA. *J. Photoch. Photobio. B* **2010,** *100* (2), 84-91.

26. (a) Duportail, G.; Lami, H., Studies of the interaction of the fluorophores harmine and harmaline with calf thymus DNA. **1975,** *402* (1), 20-30; (b) Duportail, G., Linear and circular dichroism of harmine and harmaline interacting with DNA. *Inter. J. Biol. Macromol.* **1981,** *3* (3), 188-192.

27. Laguna, A.; Aranda, S.; Barallobre, M. J.; Barhoum, R.; Fernández, E.; Fotaki, V.; Delabar, J. M.; de la Luna, S.; de la Villa, P.; Arbonés, M. L., The Protein Kinase DYRK1A Regulates Caspase-9-Mediated Apoptosis during Retina Development. *Dev. Cell* **2008,** *15* (6), 841-853.

28. Ma, Y.; Wink, M., The beta-carboline alkaloid harmine inhibits BCRP and can reverse resistance to the anticancer drugs mitoxantrone and camptothecin in breast cancer cells. *Phytother. Res.* **2010,** *24* (1), 146-149.

29. Dias, A.; Varela, A. P.; Miguel, M. d. G.; Macanita, A. L.; Becker, R. S., .beta.-Carboline photosensitizers. 1. Photophysics, kinetics and excited-state equilibria in organic solvents, and theoretical calculations. *J. Phys. Chem.* **1992,** *96* (25), 10290-10296.

30. Dias, A.; Varela, A. P.; da Graça Miguel, M.; Becker, R. S.; Burrows, H. D.; Maçanita, A. L., β-Carbolines. 2. Rate Constants of Proton Transfer from Multiexponential Decays in the Lowest Singlet Excited State of Harmine in Water As a Function of pH. *J. Phys. Chem.* **1996,** *100* (45), 17970-17977.

31. (a) Fukuzumi, S.; Miyao, H.; Ohkubo, K.; Suenobu, T., Electron-Transfer Oxidation Properties of DNA Bases and DNA Oligomers. *J. Phys. Chem. A* **2005,** *109* (15), 3285-3294; (b) Crespo-Hernández, C. E.; Close, D. M.; Gorb, L.; Leszczynski, J., Determination of Redox Potentials for the Watson−Crick Base Pairs, DNA Nucleosides, and Relevant Nucleoside Analogues. *J. Phys. Chem. B* **2007,** *111* (19), 5386-5395.

32. Kalyanasundaram, K.; Gratzel, M., Proflavine-sensitized photoproduction of H2 from water with electron-donors and a colloidal redox catalyst. *J. Chem. Soc., Chem. Commun.* **1979,** (24), 1137-1138.

33. Sasikala, W. D.; Mukherjee, A., Molecular Mechanism of Direct Proflavine–DNA Intercalation: Evidence for Drug-Induced Minimum Base-Stacking Penalty Pathway. *J. Phys. Chem. B* **2012,** *116* (40), 12208-12212.

34. Ingersoll, C. M.; Strollo, C. M., Steady State Fluorescence Anisotropy to Investigate Flavonoids Binding to Proteins. *J. Chem. Educ.* **2007,** *84*, 1313-1315.

35. Lakowicz, J. R., Principles of Fluorescence Spectroscopy. *springer* **2006,** *Third Edition*.

36. Fleming, G. R., Chemical application of ultrafast spectroscopy. *Oxford unversity Press, New York* **1986**.

37. (a) Zsila, F.; Bikadi, Z.; Simonyi, M., Circular dichroism spectroscopic studies reveal pH dependent binding of curcumin in the minor groove of natural and synthetic nucleic acids. *Org. Biomolec. Chem.* **2004,** *2* (20), 2902-2910; (b) JOUR; Kypr, J.; Kejnovská, I.; Renciuk, D.; Vorlícková, M., Circular dichroism and conformational polymorphism of DNA. *Nucleic Acids Res.* **2009,** *37* (6), 1713 -1725

38. (a) Ghosh, S.; Kar, A.; Chowdhury, S.; Dasgupta, D., Ellipticine Binds to a Human Telomere Sequence: An Additional Mode of Action as a Putative Anticancer Agent? *Biochemistry* **2013,** *52* (24), 4127-4137; (b) Rujan, I. N.; Meleney, J. C.; Bolton, P. H., Vertebrate telomere repeat DNAs favor external loop propeller quadruplex structures in the presence of high concentrations of potassium. *Nucleic Acids Res.* **2005,** *33* (6), 2022-2031.

39. Koeppel, F.; Riou, J.-F.; Laoui, A.; Mailliet, P.; Arimondo, P. B.; Labit, D.; Petitgenet, O.; Hélène, C.; Mergny, J.-L., Ethidium derivatives bind to G-quartets, inhibit telomerase and act as fluorescent probes for quadruplexes. *Nucleic Acids Res.* **2001,** *29* (5), 1087-1096.

40. Wiseman, T.; Williston, S.; Brandts, J. F.; Lin, L.-N., Rapid measurement of binding constants and heats of binding using a new titration calorimeter. *Anal. Biochem.* **1989,** *179* (1), 131-137.

41. (a) Barbieri, C. M.; Srinivasan, A. R.; Rzuczek, S. G.; Rice, J. E.; LaVoie, E. J.; Pilch, D. S., Defining the mode, energetics and specificity with which a macrocyclic hexaoxazole binds to human telomeric G-quadruplex DNA. *Nucleic Acids Res.* **2007,** *35* (10), 3272-3286; (b) Pilch, D. S.; Barbieri, C. M.; Rzuczek, S. G.; LaVoie, E. J.; Rice, J. E., Targeting human telomeric G-quadruplex DNA with oxazole-containing macrocyclic compounds. *Biochimie* **2008,** *90* (8), 1233-1249.

42. Buck, A. T.; Paletta, J. T.; Khindurangala, S. A.; Beck, C. L.; Winter, A. H., A Noncovalently Reversible Paramagnetic Switch in Water. *J. Am. Chem. Soc.* **2013,** *135* (29), 10594-10597.

43. Wei, C.; Jia, G.; Yuan, J.; Feng, Z.; Li, C., A Spectroscopic Study on the Interactions of Porphyrin with G-Quadruplex DNAs†. *Biochemistry* **2006,** *45* (21), 6681-6691.

44. Bai, L.-P.; Ho, H.-M.; Ma, D.-L.; Yang, H.; Fu, W.-C.; Jiang, Z.-H., Aminoglycosylation Can Enhance the G-Quadruplex Binding Activity of Epigallocatechin. *PLoS ONE* **2013,** *8* (1), e53962.

45. (a) Bazzicalupi, C.; Ferraroni, M.; Bilia, A. R.; Scheggi, F.; Gratteri, P., The crystal structure of human telomeric DNA complexed with berberine: an interesting case of stacked ligand to G-tetrad ratio higher than 1:1. *Nucleic Acids Res.* **2013,** *41* (1), 632-638; (b) Pradhan, S. K.; Dasgupta, D.; Basu, G., Human telomere d[(TTAGGG)4] undergoes a conformational transition to the Na+-form upon binding

with sanguinarine in presence of K+. *Biochem. Bioph. Res. Comm.* **2011,** *404* (1), 139-142.

46. Tan, J.-H.; Ou, T.-M.; Hou, J.-Q.; Lu, Y.-J.; Huang, S.-L.; Luo, H.-B.; Wu, J.-Y.; Huang, Z.-S.; Wong, K.-Y.; Gu, L.-Q., Isaindigotone Derivatives: A New Class of Highly Selective Ligands for Telomeric G-Quadruplex DNA. *J. Med.Chem.* **2009,** *52* (9), 2825-2835.

47. Zhang, F.; Goyal, R. N.; Blank, C. L.; Dryhurst, G., Oxidation chemistry and biochemistry of the central mammalian alkaloid 1-methyl-6-hydroxy-1,2,3,4-tetrahydro-.beta.-carboline. *J. Med.Chem.* **1992,** *35* (1), 82-93.